Published in final edited form as:

Dev Cell. 2015 July 6; 34(1): 45–57. doi:10.1016/j.devcel.2015.05.011.

Chloroplast stromules function during innate immunity

Jeffrey L. Caplan[‡,*], **Amutha Sampath Kumar**[‡], **Eunsook Park**[†], **Meenu S. Padmanabhan**[†], **Kyle Hoban**[‡], **Shannon Modla**[‡], **Kirk Czymmek**[‡], and **S. P. Dinesh-Kumar**[†,*]

[†]Department of Plant Biology and The Genome Center, College of Biological Sciences, University of California, Davis, CA 95616

[‡]Department of Biological Sciences, Delaware Biotechnology Institute, University of Delaware, Newark, DE 19711

Summary

Inter-organellar communication is vital for successful innate immune responses that confer defense against pathogens. However, little is known about how chloroplasts, which are a major production site of pro-defense molecules, communicate and coordinate with other organelles during defense. Here we show that chloroplasts send out dynamic tubular extensions called stromules during innate immunity or exogenous application of the pro-defense signals, hydrogen peroxide (H_2O_2) and salicylic acid (SA). Interestingly, numerous stromules surround nuclei during defense response and these connections correlate with an accumulation of chloroplast-localized NRIP1 defense protein and H_2O_2 in the nucleus. Furthermore, silencing and knockout of *CHloroplast Unusual Positioning 1* (*CHUP1*) that encodes a chloroplast outer envelope protein constitutively induces stromules in the absence of pathogen infection and enhances programmed cell death (PCD). These results support a model in which stromules aid in the amplification and/or transport of pro-defense signals into the nucleus and other subcellular compartments during immunity.

Abstract

[*]Correspondence: spdineshkumar@ucdavis.edu (Phone: 530-752-2205; Fax: 530-752-5410). jcaplan@udel.edu (Phone: 302-831-3403; Fax: 302-831-4841).

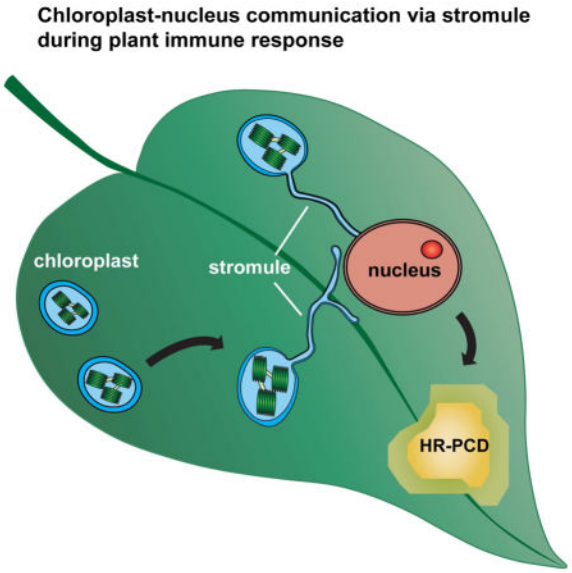

Introduction

Plant intracellular nucleotide-binding-leucine rich repeat (NLR) classes of immune receptors have structural similarity with mammalian NOD-like receptors (Caplan et al., 2008a; Ting et al., 2008). Some plant NLRs possess a coil-coiled (CC) domain while others contain a Toll-Interleukin-1 receptor homology Region (TIR) at N termini (Caplan et al., 2008a). Unlike mammalian NLRs that recognize conserved pathogen-associated molecular patterns (PAMPs), each plant NLR recognizes a specific pathogen-encoded effector protein either directly or indirectly.

Plant NLR recognition of effectors often leads to the induction of a specialized form of programmed cell death (PCD) called the hypersensitive response (HR) at the infection site and restricts pathogen spread (Mur et al., 2008). The HR-PCD onset is preceded by production of pro-PCD signals such as salicylic acid (SA), nitric oxide (NO), and reactive oxygen species (ROS) that includes superoxide (O_2^-) and hydrogen peroxide (H_2O_2) (Mur et al., 2008). It has been proposed that H_2O_2 produced during the early phase of immune response induces SA synthesis at the site of infection and this increased SA level potentiates further H_2O_2 production in a self-amplifying feedback loop (Vlot et al., 2009).

In vertebrate animals, mitochondria are the main source of pro-death signals (Wang and Youle, 2009). However, in plants, most of the corollary pathways are absent, suggesting that initiation and control of PCD is mediated by alternative mechanism(s). In addition to mitochondria, plants have various forms of plastids, such as chloroplasts. Chloroplasts are a major source of pro-PCD signals such as ROS, NO, and SA. The ROS, H_2O_2, during HR-PCD can also originate from plasma membrane localized respiratory burst oxidase homologs (RBOH) of NADPH oxidase (Torres et al., 2006). However, it appears that intracellular ROS during HR-PCD is mainly generated through chloroplasts in a light-dependent manner (Shapiguzov et al., 2012) and chloroplast-generated H_2O_2 signals through MAPK cascades (Liu et al., 2007).

We have shown that N TIR-NLR receptor recognition of p50 effector from *Tobacco Mosaic Virus* (TMV) requires the chloroplastic N Receptor Interacting Protein 1 (NRIP1) (Caplan et al., 2008b). NRIP1 localizes to chloroplasts in unchallenged N plants. Upon infection with TMV, NRIP1 is recruited from chloroplasts to the cytosol and nucleus via an unknown mechanism (Caplan et al., 2008b). In these studies, we made an initial observation that chloroplasts send out dynamic tubular projections known as “stromules” during an N-mediated defense, suggesting that chloroplasts have an additional function downstream of pathogen recognition.

Stromules are stroma filled tubules that extend from all types of plastids, including proplastids, chloroplasts, amyloplasts, etioplasts, and chromoplasts (reviewed in Natesan et al., 2005). Stromules are dynamic structures that extend along actin microfilaments and the endoplasmic reticulum (ER) (Hanson and Sattarzadeh, 2011; Schattat et al., 2011). Stromules can connect plastids and provide a means of exchange of stromal components between plastids; however, it appears that this is a rare event and not their main function (Hanson and Sattarzadeh, 2013; Mathur et al., 2013; Schattat et al., 2012). Stromules can closely associate with the plasma membrane, mitochondria, and nuclei, but the function of these connections is unknown (Hanson and Sattarzadeh, 2011; Schattat et al., 2011). Stromules are induced during mycorrhizae symbiosis with plants, starch granule formation, sucrose or glucose application, and abotic and biotic stresses (reviewed in Kumar et al., 2014). Although stromules were first described over 50 years ago (Esau, 1944; Shalla, 1964), their biological function remains elusive.

Here we show that chloroplastic stromules are strongly induced during immune response in *Arabidopsis* and *Nicotiana* plants. Stromules are induced during the beginning phases of HR-PCD initiated by viral and bacterial effectors. Our quantitative data show that stromules are also induced along the borders of the HR-PCD site indicating that pro-PCD cell-to-cell signal(s) may induce stromule formation. Interestingly, exogenous application of pro-PCD signals such as H_2O_2 and SA was sufficient to induce stromules. During immune response, we observed strong stromule-to-nuclei connections that preceded the accumulation of chloroplast-localized NRIP1-Cerulean protein in the nucleus. In addition, we observed increased H_2O_2 in the nucleus at the connection sites of stromules and nuclei. These data provide evidence that stromule-to-nuclei connections are involved in the signaling from chloroplasts-to-nuclei during a defense response. Furthermore, we show that constitutive induction of stromules enhances HR-PCD, proving that stromules function during the progression of HR-PCD. We propose a model in which stromules are involved in transducing and amplifying pro-defense signals originating from chloroplasts.

Results

Dynamic chloroplast stromule extensions are induced during N-mediated viral defense

The N TIR-NLR recognizes the p50 helicase domain of TMV replicases and activates signaling leading to HR-PCD and containment of the virus to the infection site. During p50 initiated defense, chloroplast localized NRIP1 is recruited from chloroplasts to the cytosol and nucleus via an unknown mechanism (Caplan et al., 2008b). Since NRIP1 plays an important role in pathogen recognition, we investigated the dynamics of NRIP1 localization

during immune response. Interestingly, we observed strong induction of highly dynamic tubular projections from chloroplasts called stromules during p50-induced HR-PCD (Figure 1A). These results confirmed our previous preliminary observation that stromules are induced during N-mediated defense against TMV (Caplan et al., 2008b).

To quantitatively study stromule induction during HR-PCD, we first optimized a method using confocal laser scanning microscopy (CLSM) to obtain fast z-stacks through epidermal cells. Epidermal cells are relatively flat compared to mesophyll cells and their chloroplasts are smaller, less numerous, and spread out; therefore, it is easier to estimate the number of stromules from 2D maximum intensity projections of their 3D volumes. Other studies have used epidermal chloroplasts to study stromules (Natesan et al., 2009). Using this optimized method, we quantified stromule induction in N and NRIP1-Cerulean expressing transgenic *N. benthamiana* plants (Caplan et al., 2008b). We expressed p50 using Agrobacterium-mediated transient assay rather than inoculation with TMV so that the function of stromules during HR-PCD can be examined independently from the complex effects of viral pathogenesis (Krenz et al., 2012). We observed a strong induction of the total number of stromules per total number of chloroplasts in N plants expressing p50 fused to Citrine (p50-Citrine) at 46 h compared to Citrine control (Figure 1B). This occurs after N recognition of p50 at 42–46 h post expression of p50 (Padmanabhan et al., 2013) and this timeframe is consistent with the beginning phase of HR-PCD induction during N-mediated defense. Plants without the N cannot recognize p50, and hence, failed to induce HR-PCD. Consistent with this, stromule induction was significantly reduced in the plants without N upon expression of p50-Citrine (Figure 1B). Furthermore, there was a significant induction of stromules in the abaxial mesophyll cells of N plants expressing p50 fused to a tandem affinity purification tag (p50-TAP) compared to the TAP control (Figure 1C and D), suggesting the induction is not specific to epidermal chloroplasts. These results clearly indicated that stromules were induced significantly during HR-PCD response to a viral effector and not caused by the viral infection.

Stromules are induced during bacterial immune response

Next, we examined if this is a common response during defense. For this, we examined pepper BS2 CC-NLR that recognizes *Xanthomonas campestris* effector AvrBS2 and activates HR-PCD and defense (Leister et al., 2005). Since transient coexpression of BS2 and AvrBS2 in *N. benthamiana* induces HR-PCD (Leister et al., 2005), we tested for stromule induction using NRIP1-Cerulean transgenic plants. NRIP1-Cerulean served as a marker to monitor stromules and NRIP1 has no known function in BS2 responses. At 48 h post coexpression of BS2 and AvrBS2, we observed a strong induction of stromules compared to the BS2 alone control (Figure 2A). To further extend these results, we examined *Pseudomonas syringe* bacterial effectors AvrB and AvrRpt2 that induce HR-PCD in *N. benthamiana* and found transient expression of avrB and AvrRpt2 induces stromules (Figure S1A). These results indicated that stromules were also induced during bacterial immune response.

In Arabidopsis Col-0 plants, RPS4 TIR-NLR and RPS2 and RPM1 CC-NLRs recognize *P. syringae pv tomato* DC3000 strain (*Pst*) expressing AvrRps4, AvrRpt2, and AvrRpm1

effectors respectively and activate defense response. To investigate if stromule induction also occurs in Arabidopsis, we generated homozygous transgenic Col-0 plants expressing NRIP1-Cerulean. NRIP1-Cerulean served as a marker to monitor stromules and NRIP1 has no known function in RPS4, RPS2, and RPM1-mediated responses. We observed significant induction of stromules at 6 h post-infection with *Pst::AvrRpt2* and *Pst::AvrRpm1* and at 24 h post-infection with *Pst::AvrRps4* compared to the control (Figure 2B and C). These data were confirmed in another Col-0 marker line that expresses RecA chloroplast-transit peptide fused to GFP (cTP-GFP) (Kohler et al., 1997); we observed significant induction of stromules in response to *Pst::AvrRps4* and *Pst::AvrRpt2* infection (Figure S1B and C). These results indicate that stromules are specifically induced in respnse to effector-triggred immunity (ETI).

To determine if stromule induction is dependent on the presence of the effector, we infected Col-0 NRIP1-Cerulean plants with *Pst* that is unable to activate ETI and with the *Pst hrcC* mutant that fails to deliver effectors into plant cells. We observed no significant induction of stromules in response to both *Pst* strains compared to control (Figure 2D and E). Both *Pst* and *Pst hrcC* still activate PAMP-triggered immunity (PTI), suggesting PTI do not induce stromules (Mansfiled, 2009). However, when PTI was activated by direct treatment with flg22 peptide, we observed significant induction of stromules (Figure S1D and E). The stromule induction is dynamic with significant induction at 0.5 h, reduced induction at 2 h and then increased induction at 8 h post-flg22 treatment (Figure S1D and E). We hypothesize that the observed induction at 0.5 h may be related to ROS burst that occurs early during flg22-mediated response (Smith and Heese, 2014). Together, these results indicate that stromule induction is a general response during both viral and bacterial immune response.

Stromules are induced at the site and along the borders of the HR-PCD site

HR-PCD induced during N-mediated defense spreads beyond the initial site of TMV infection. As a result, there are three distinct zones in infected tissue: inside the initial HR-PCD infection site, the border surrounding the initial HR-PCD site, and far outside of HR-PCD. We determined if stromules are induced in these zones by expressing p50-Citrine. Since TMV itself can spread from the initial infection site, we did not use TMV because this would have confounded the effect on the movement of signal from the HR-PCD site. Interestingly, we observed a strong induction of stromules inside and a moderate induction along the borders of HR-PCD, but no induction far outside the HR-PCD site (Figure 3A and B). Induction of stromules along the borders of the infection site suggests that a cell-to-cell signal originating during the HR-PCD can induce stromule formation.

Pro-defense signaling molecules SA and H_2O_2 induce stromules

ROS (H_2O_2 and O_2^-), NO, and SA synthesis occurs in chloroplasts and they are significantly induced during defense. It is possible that these pro-defense molecules are responsible for cell-to-cell signaling that induces stromules along the borders of HR-PCD. Therefore we tested whether exogenous application of these molecules can induce stromules. Stromules were not induced in *N. benthamiana* plants infiltrated with buffer (mock), NO donor SNAP, and O_2^- generated by xanthine plus xanthine oxidase (Figure 3C

and D). However, application of H_2O_2 and the SA analog, INA, resulted in stromule induction (Figure 3C and D). INA and H_2O_2 can also induce stromules in *Arabidopsis* cTP-GFP plants compared to mock control (Figure S2A). To further extend these observations, we tested if stromules could be induced in Arabidopsis mesophyll protoplasts and observed significant induction as early as 1 h post-treatment with SA (Figure S2B and C). These results indicate that exogenous application of H_2O_2 and SA pro-defense molecules is sufficient to induce stromules. Therefore, H_2O_2 and/or SA induced during immune response could serve as signals for stromule induction.

Stromules form numerous connections with nuclei during immune response

Stromules can also associate with the membranes of other organelles, such as the ER, plasma membrane and nuclei (Hanson and Sattarzadeh, 2011; Schattat et al., 2011). Interestingly, we discovered that stromules form numerous nuclei connections during p50-induced defense in N plants (Figure 4A and B). We observed the tip of stromules connecting directly to nuclei or the body of the chloroplast associating with nuclei (Figure 4A, top row; columns 2 and 4) compared to the control (Figure 4A, bottom row). In addition, we observed stromules wrapped around nuclei (Figure 4B, top left panel), multiple stromule ends tethered to nuclei (Figure 4B, top right panel), and complex mixtures of associations (Figure 4B, bottom panels). Estimations of stromule-to-nuclei connections conducted manually from CLSM z-stacks showed significant increase in chloroplast-to-nuclei connections during a p50-induced defense (Figure 4C). The clustering of chloroplasts around nuclei was also induced by INA and by BS2-mediated HR-PCD (Figure S3). Time-lapsed and 3D projection movies (Movie S1 and S2) reveal that these associations can be a tight tethering between the chloroplast outer membrane and the nuclear envelope.

The stromule-to-nuclear connections suggest that stromules may be involved in chloroplast-to-nuclear transport of signals, which would require a tigh association to nuclei. To examine this, we conducted correlative light and electron microscopy (CLEM). We transiently expressed p50-Citrine in N plants to induce HR-PCD and stromule-to-nuclear connections. Small leaf excisions were fixed and imaged on CLSM (Figure 5A; left panel) and then embedded for transmission electron microscopy (TEM). The exact same nucleus imaged by CLSM was relocated and imaged on the TEM (Figure 5A; middle panel). TEM micrographs confirmed different types of tight associations between stromules and nucleus during HR-PCD (Figure 5B–E). The tip of a stromule and the body of the chloroplast were observed in close proximity to the nuclear envelope (Figure 5B and C). Cross-sections of stromules that wrapped around the nucleus were found in nuclear grooves (Figure 5D), where the nuclear envelope partially surrounded the stromule. The chloroplast and nuclear membranes appeared in close proximity, but were not tightly associated, suggesting that a direct membrane-to-membrane interaction does not drive stromules and chloroplasts to nuclei, but rather, the phenomenon is more likely directed by an interaction with the cytoskeleton. The membranes appeared perforated at the association sites (Figure 5C and D, arrowheads), but it is difficult to conclude if the perforations were nuclear pores. However, slightly oblique sections show that stromules are in close proximity to nuclear pores along the nuclear envelope (Figure 5E, arrows). Collectively these results indicate that during immune response there is significant induction of stromule to nuclear connections.

NRIP1 accumulate in nuclei during immunity

The observed stromules to nuclei associations suggest exchange of signaling molecules between chloroplast and nucleus. Interestingly, nuclei that had established connections with stromules or clustering of chloroplasts around nuclei showed an increased NRIP1-Cerulean accumulation in the nuclei during p50-induced defense (Figure 4A). These results suggest that the induction of stromules and stromule-to-nuclei associations provides a possible mechanism for the increase of NRIP1-Cerulean in nuclei during N-mediated HR-PCD (Caplan et al., 2008b).

This strongly induced stromule-to-nuclear associations and accumulation of NRIP1-Cerulean in nuclei was also observed during HR-PCD induced by transient coexpression of BS2 and AvrBS2 effector, suggesting the movement/transport appears to be a general response during HR-PCD (Figure S3, left panel). In addition, stromules induced by the SA analog, INA, resulted in the clustering of chloroplasts around nuclei and the accumulation of NRIP1-Cerulean within nuclei (Figure S3, right panel). Since the concentration of INA used here does not induce macroscopic HR-PCD, these results suggest that the accumulation of chloroplastic NRIP1-Cerulean in nuclei does not require the onset of HR-PCD, but rather, only requires chloroplast-to-nuclear associations.

Chloroplast-targeted proteins may accumulate in the nucleus by either a disruption of import into chloroplasts or by a movement of protein out of chloroplasts possibly via chloroplast-to-nuclear associations. Western blot detection of chloroplast-derived proteins in the nucleus is extremely challenging because it is difficult to obtain nuclear extracts completely free of chloroplast contamination (Sikorskaite et al., 2013). Therefore, to distinguish between these two modes of accumulation, we designed an experimental strategy that uses a nuclear export sequence (NES) from *human immunodeficiency virus* (HIV) Rev protein fused to NRIP1-Cerulean (Figure 6A). If protein import into chloroplasts is disrupted, then NES-NRIP1-Cerulean will retain the NES and will be driven into the cytosol by the NES (Figure 6A, left panel). If NES-NRIP1-Cerulean is imported into the chloroplasts, it will be processed and the NES will be cleaved off with the chloroplast transit peptide (cTP) (Figure 6A, right panel). Then, if that fraction of processed NRIP1-Cerulean moves out of the chloroplasts, it will lack the NES, and therefore, could accumulate in the nucleus.

To test this approach, we first determined the functionality of the NES by fusing it to Cerulean (Cerulean-NES). Cerulean-NES expression in *N. benthamiana* showed Cerulean fluorescence that was largely excluded from nuclei (Figure 6B). Furthermore, addition of NES to the N-terminus of NRIP1-Cerulean did not disrupt import of NES-NRIP1-Cerulean into chloroplasts because we observed strong Cerulean fluorescence in the chloroplasts (Figure 6C). To test if NES-NRIP1-Cerulean accumulates in the nucleus during the p50-mediated HR-PCD, we generated a control in which the order of the NES, NRIP1(cTP), and Cerulean were switched to form Cerulean-NRIP1(cTP)-NES, a fusion that will not be targeted to the chloroplasts. Both NES-NRIP1-Cerulean and Cerulean-NRIP1(cTP)-NES were expressed with p50-TAP for 36 h. Cerulean fluorescence was largely excluded from nucleus in cells expressing Cerulean-NRIP1(cTP)-NES control (Figure 6D, left panels). In contrast, in cells expressing the NES-NRIP1-Cerulean, we observed enhanced Cerulean

fluorescence in the nuclei that had stromule-to-nuclear connections (Figure 6D, right panels). These results suggest that NES-NRIP1-Cerulean was first targeted to the chloroplast where the NES-cTP portion was cleaved off and only the remaining NRIP1-Ceulean moved out of the chloroplasts and accumulated in the nucleus. The advantage of this approach is that it can detect very low levels of NRIP1-Cerulean accumulation in the nucleus. Quantification showed a high ratio of nuclear-to-cytosolic fluorescence in NES-NRIP1-Cerulean expressing cells (Figure 6E, 2) compared to the Cerulean-NRIP1(cTP)-NES (Figure 6E, 1). These results clearly demonstrate that the NRIP1 moves from chloroplast and accumulates in the nucleus during immune response.

H_2O_2 accumulate in nuclei during immunity

Since chloroplast-to-nuclear connections correlated with the movement of NRIP1-Cerulean to nuclei, we hypothesized that pro-defense molecules such as H_2O_2, may also move from chloroplasts-to-nuclei via stromule connections. We tested this by monitoring H_2O_2 levels using the genetically encoded HyPer sensor (Belousov et al., 2006). HyPer detection of H_2O_2 is ratiometric and not fluorescence intensity-based like most H_2O_2 dyes, making it better for comparing H_2O_2 in different subcellular locations. We targeted HyPer to the chloroplasts by fusing the *Arabidopsis* RecA chloroplast-transit peptide (RecA(cTP)-HyPer). The RecA(cTP)-HyPer was expressed and then a defense response was subsequently induced by p50-TAP expression. Since it takes approximately 16–18 h for transient expression to begin, we started the time course at 19 h post-p50-TAP infiltration. Although our intention was to conduct this experiment as a live time course, the laser excitation for the sensor rapidly induced H_2O_2 in the chloroplasts. Therefore, we viewed leaf sections using infrared light and only single CLSM images were taken for each time points between 19 to 48 h. Using this approach, we observed a strong H_2O_2 burst at 28 h confirming directly that chloroplasts are a significant source of H_2O_2 during HR-PCD (Figure 6F and G).

The association of stromules and the body of chloroplasts with nuclei led us to study H_2O_2 movement from chloroplasts to nuclei by coexpressing RecA(cTP)-HyPer and p50-TAP. Similar to the accumulation of NRIP1-Cerulean in the nucleus and cytosol during a defense response, we observed the RecA(cTP)-HyPer accumulation in these locations in addition to chloroplasts, which made it possible to examine H_2O_2 concentrations in all of these subcellular locations (Figure 6H). Furthermore, a large amount of H_2O_2 was seen at the interface of chloroplasts-to-nuclear connections and appeared as a gradient emanating from the body of the chloroplast into the nucleus (Figure 6H) (Movie S3). The unidirectional nature of the gradients, rather than uniformly distributed fluorescence, suggests that we were detecting H_2O_2 and not just out of focus light.

To further rule out the possibility of technical artifacts, we targeted HyPer to the nucleus by fusing to a nuclear localization signal (NLS-HyPer). This allowed us to detect ROS specifically in the nucleus. A controlled ROS burst in chloroplasts surrounding nuclei at the region of interest was induced with the 405 nm laser. An increase in ROS within nuclei was observed after ROS induction in the chloroplasts (Figure 6I), suggesting ROS generated in chloroplasts can move into adjacent nuclei. These results suggest that a possible function of

stromules, and more broadly chloroplast-to-nuclear connections, is to aid in the transport of signaling molecules such as H_2O_2 during defense.

Disruption of chloroplast outer envelope proteins abolishes stromule induction

Little is known about the genetic components that are required for stromule formation. It has been shown that stromules extend along actin microfilaments (Kwok and Hanson, 2004), suggesting a role for chloroplast outer envelope membrane proteins (OEPs) that associate with actin. The nuclear encoded Chloroplast Unusual Positioning 1 (CHUP1) is required for chloroplast movement, targeted to the chloroplast outer envelope membrane and contains an actin-binding domain (Kadota et al., 2009; Schmidt von Braun and Schleiff, 2008). Overexpression of CHUP1 or OEP7 targeting peptides saturates the chloroplast insertion machinery and disrupts other proteins using the same insertion mechanism (Oikawa et al., 2008). To investigate if disrupting OEPs prevents stromule formation, we transiently overexpressed the CHUP1 target peptide (cTP) fused with TagRFP [CHUP1(cTP)-tRFP] in transgenic NRIP1-Cerulean plants containing N. After 42 h post CHUP1(cTP)-tRFP overexpression, we observed an almost complete loss of stromule induction during p50-Citrine-mediated HR-PCD (Figure 7A and B). These results suggest that either CHUP1 itself or other OEPs are required for stromule formation.

CHUP1 silencing and knockout leads to constitutive stromule induction and accelerates HR-PCD

Overexpression of CHUP1(cTP)-tRFP longer than 42 h led to clustering of chloroplasts, long tubule connections between chloroplasts, and eventually cell death (Figure S4). Therefore, it was not possible to use this approach to assess the effect on HR-PCD. Instead, we knocked down *CHUP1* expression using virus induced gene silencing (VIGS) (Liu et al., 2002). Interestingly, rather than disrupting stromules, we observed a constitutive induction of stromules in *CHUP1*-silenced plants compared to the control (Figure 7C and D). These results suggest that CHUP1 itself is not required for stromule formation. The function of CHUP1 in regulating stromules is unclear; however, this unexpected CHUP1 phenotype provided a unique opportunity to test our model. The data described above show that H_2O_2 induced stromules and chloroplast-to-nuclear associations can aid in the movement of H_2O_2 to nuclei. As a result, we propose that stromules function during the amplification of pro-defense signals, such as H_2O_2 and possibly SA, to overcome the threshold required for HR-PCD signaling. If stromules function during this amplification loop, then a constitutive induction of stromules should enhance HR-PCD. Indeed, the HR-PCD was enhanced in the *CHUP1*-silenced plants compared to the control (Figure 7E).

To determine if Arabiodpsis *chup1* kncokout plants exhibit similar phenotype as CHUP1-silencing, we generated *chup1* knockout line described in (Schmidt von Braun and Schleiff, 2008) expressing NRIP1-Cerulean marker. Similar to CHUP1-silencing, *chup1* knockout plants also exhibit constitutive stromules compared to Col-0 control (Figure 7F and G). Furthermore, the HR-PCD was enhanced in *chup1* plants infected with *Pst::AvrRpt2* compared to Col-0 (Figure 7H and I). Collectively, these results indicate that stromules enhance HR-PCD.

Discussion

We show that chloroplasts dynamically change their morphology by sending out stromule extensions during defense response. Since pro-defense signals such as H_2O_2 and SA originate from chloroplasts, the increase in surface area of tubule extensions may aid in the transfer of these signals and/or other signaling proteins or metabolites to the cytosol and nucleus where they function to activate defense signaling. Indeed, we observed stromules forming complex associations surrounding nuclei during HR-PCD and subsequent clustering of chloroplasts around nuclei. Our data also show that H_2O_2 and SA can induce stromule formation and H_2O_2 can move through these chloroplast-to-nuclear connections. Using our NES fusion approach, we show that a chloroplast-localized NRIP1 accumulates in the nucleus during immune response possibly via chloroplast-to-nuclear associations. Constitutive induction of stromules by silencing or knockout of chloroplast outer envelope protein CHUP1 enhanced HR-PCD. Consequently, we propose an amplification model in which stromules and pro-HR-PCD signals form a positive feedback loop.

The biological function of stromules has remained elusive despite being described 50 years ago (Esau, 1944; Shalla, 1964). Here, we showed that stromules have a function during ETI. We demonstrated induction of stromules during ETI in multiple ways. First, we uncoupled the known viral induction of stromules from ETI, by expressing p50 in N plants to specifically induce HR-PCD. These experiments showed a dramatic increase in stromule formation. Second, stromule induction was highly specific to *Pst* bacteria expressing effectors that activate ETI and was confirmed using two independent stromule marker lines. Stromules were not induced in the *Pst* or *Pst hrcC* mutant that fails to deliver effectors. However, direct treatment with flg22 can induce stromules indicating that robust PTI response can also induce stromule formation. Combined with our data showing that constitutive induction of stromules accelerates HR-PCD, this study clearly demonstrates that stromule induction plays an important role in the progression of HR-PCD during ETI. Our data suggests stromules may have a role during flg22-mediated response and furture in-depth studies will need to be conducted to clearly define the role of stromules during PTI.

H_2O_2 is induced as a biphasic burst during HR-PCD (Lamb and Dixon, 1997). Stromules are unlikely to play a role during the initial burst, since their formation over minutes to hours is dynamically too slow. Instead, they are more likely to function during the second phase of ROS burst that occurs over hours. Chloroplasts are the main source of sustained H_2O_2 and other forms of ROS burst during HR-PCD (Zurbriggen et al., 2010) and light-dependent H_2O_2 from chloroplasts is important for HR-PCD (Liu et al., 2007). Therefore, we propose that chloroplast generated H_2O_2 and SA form the secondary burst, and stromules are required for H_2O_2 and SA levels in the cytosol and nucleus to reach the threshold for inducing HR-PCD and defense. Cell-to-cell signaling or even movement of H_2O_2 and SA may contribute to reaching a threshold level for HR-PCD. Indeed, we observed stromule induction outside of the intial HR-PCD site (Figure 3), suggesting that stromules are likely a result of intra- and inter-cellular signal perception.

Our observations suggest that during HR-PCD, chloroplasts progresses from stromule induction, stromule-to-nuclear connections, chloroplast clustering around nucleus, and

lastly, movement and accumulation of NRIP1-Cerulean and H_2O_2 in the nucleus. We have observed stromules contracting and resulting in the body of the chloroplast associating with nuclei; however, it is unclear if these stromules are pulling, guiding, or just compressed during the movement of chloroplasts to nuclei. In any case, it is clear that there is a direct correlation between chloroplast clustering around nuclei and the enhanced accumulation of chloroplast-localized NRIP1-Cerulean in the nuclei.

Controlled stromule-to-nuclei connections may provide a means of regulated movement of pro-defense signals such as H_2O_2 to poise the cell for rapid induction of HR-PCD and/or defense gene induction in the neighboring uninfected cells surrounding HR-PCD site. Chloroplastic clustering may be a more efficient mode of movement of pro-defense signals, and once this stage is reached, HR-PCD is more likely imminent at the site of infection. Interestingly, chloroplast clustering can be induced by some strains of Agrobacterium, suggesting that clustering alone is not sufficient to induce HR-PCD (Erickson et al., 2014). Our studies described here with the HyPer sensor supports this model by showing a gradient of H_2O_2 emanating from a chloroplast associated with a nucleus and accumulation of chloroplast-generated H_2O_2 in nuclei. This direct evidence suggests that stromules may be involved in retrograde chloroplast-to-nuclear signaling. Interestingly, mitochondria cluster around nuclei in mammalian cells during hypoxia results in an increase in ROS accumulation in the nucleus and direct modifications of promoter sequences (Al-Mehdi et al., 2012).

It is easy to comprehend how stromule-to-nuclei and other chloroplast-to-nuclear connections can aid in the transport of small signaling molecules such as H_2O_2. To move from the chloroplast stroma, H_2O_2 must move across the inner chloroplast membrane, the outer chloroplast membrane and the nuclear envelope to finally arrive in the nucleus. H_2O_2 cannot freely diffuse across the chloroplast envelope membranes and instead uses aquaporins (Mubarakshina Borisova et al., 2012). H_2O_2 most likely moves across the nuclear envelope through nuclear pores, which appear to be in close proximity to stromules (Figure 5E). In contrast, it is currently unclear how a protein, such as NRIP1, can move across this membrane system. However, our data shows chloroplasts processed NRIP1 can accumulate in nuclei. Further studies are needed to understand precise mechanism of chloroplast-to-nuclear protein transport.

Early during our studies, we hypothesized that CHUP1 was involved in stromule formation because a long exposure to blue laser light induced rapid movement of chloroplasts and stromule extensions (data not shown). Therefore we hypothesized that silencing CHUP1 would disrupt stromules, but discovered that it had the opposite effect of constitutively inducing stromules. It is possible that CHUP1 is a negative regulator of stromule formation and that the CHUP1-dependent actin cage of short actin filaments, known as cp-actin (Kadota et al., 2009), inhibits stromule formation. Alternatively, since CHUP1 and other OEPs are inserted into the chloroplast outer envelope via AKR2-dependent insertion machinery (Bae et al., 2008), it is possible that the knockdown of CHUP1 upregulates an unknown OEP that is a positive regulator or a key structural component required for stromule formation. Since CHUP1-silencing induces stromules, we reason that loss of stromule formation observed due to overexpression of CHUP1(cTP)-tRFP may be due to

non-specific disruption of function of other OEPs by saturating the insertion machinery. The two models for stromule extension are internal pushing by cytoskeleton-like structures along the inner envelope or external interaction of the outer envelope with the cytoskeleton or other membrane systems. The data here supports a role for the outer envelope during stromule formation.

Based on our results, we propose a model for HR-PCD during immunity that invokes a similar mechanism to mammalian mitochondrial-controlled PCD, but instead, chloroplasts are a major source of pro-PCD signals. Future studies will determine if other pro-PCD signals besides H_2O_2 and SA exit chloroplasts by a similar mitochondrial membrane permeablization mechanism seen in animals, and if there are other key protein or metabolite-based pro-PCD signals in plants that originate from chloroplasts. Furthermore, the exact nature of stromule associations with nuclei and other organelles, such as mitochondria and ER, will provide insight into how different organelles communicate and coordinate to control HR-PCD during innate immunity.

Experimental Procedures

Laser scanning confocal microscopy

A Zeiss LSM510 META, LSM5 DUO, LSM710, or LSM780 confocal microscope with a 40x C-Apochromat water immersion objective lens (NA 1.2) was used for live cell imaging. Approximately 0.5x1 cm leaf sections were used for imaging at indicated time points. The 458 nm and 514 nm laser lines of a 25mW argon laser were used to image Cerulean, Citrine, and chloroplasts respectively. Images within the same section of a figure were taken using the same confocal settings and adjusted equally. The HyPer was imaged by fast line switching of 405 nm or 488 nm laser excitation. Emission signal was collected at 491–543 nm on the GaAsP dector of a Zeiss LSM780 confocal microscope. A ratio of emission from channel 1 (488 nm excitation) and channel 2 (405 nm excitation) was calculated with the following equation: (ch1)/(ch2-50) * 1500-250.

Quantification of stromules

Stromules were quantified from z-stacks taken by confocal microscopy. Epidermal stromules marked with NRIP1-Cerulean were acquired using a 30–40 slice z-stack. 2D maximum intensity projections were generated in the Zeiss LSM browser software. Stromules and chloroplasts were counted in either ImageJ or Photoshop. Stromule induction was calculated as the total number of stromules per the total number of chloroplasts in a field of view.

Correlative Light and Transmission Electron Microscopy

Leaf excisions were fixed with 0.5% glutaraldehyde and 4% paraformaldehyde in PHEM (60mM PIPES, 25mM HEPES, 10mM EGTA, and 2mM $MgCl_2$, pH 6.9) buffer for 45 min. Samples were imaged on a Zeiss LSM780 confocal microscope using a 40x C-Apochromat water immersion objective (NA 1.2). The position was mapped via tile scanning of the entire leaf excision using a 10x Plan-Neofluar objective (NA 0.3). Samples were fixed again with 2% glutaraldehyde and 2% paraformaldehyde in PHEM buffer overnight at 4°C. Samples

was washed with 0.1M sodium cacodylate buffer pH 7.4, postfixed with 1% osmium tetroxide in in the same buffer for 2 h, and then washed with buffer and water. Samples were dehydrated in an acetone series (25%, 50%, 75%, 95%, and twice in anhydrous 100% acetone; 30 min each step) and infiltrated with Quetol 651-NSA resin. Samples were flat-embedded between a microscope slide treated with a PTFE-like spray and Aclar® film and polymerized at 60°C for 48 h. The resin-embedded sample was excised and attached to a flat-bottomed BEEM capsule using a cyanoacrylate glue. The region previously imaged by CLSM was then re-identified, and ultrathin serial sections were cut on a Reichert-Jung Ultracut E ultramicrotome and collected onto a film of 0.5% formvar using 2 × 1 single slot grids. Sections were post-stained with methanolic uranyl acetate and Reynolds' lead citrate and examined with a Zeiss Libra 120 TEM operating at 120kV. Images were acquired with a Gatan Ultrascan 1000 2k x 2k CCD.

Arabidopsis infection with *Pst*, *Pst hrcC*, and *Pst* expressing different effectors

Pst, Pst hrcC, and Pst expressing different effectors were grown on KM plates with appropriate antibiotics. The cells were harvested between 40–46 hrs; resuspended in 10mM $MgCl_2$, adjusted to $1X10^6$ cfu/mL (for *Pst* expressing effectors) and $2.5X10^5$ cfu/mL (for *Pst* and *Pst hrcC* expressing effectors) and infiltrated onto four-week old NRIP1-Cerulean Arabidopsis or or cTP-GFP Col-0 Arabidopsis plants (Kohler et al., 1997). Infiltrated leaves were analyzed for stromule induction at indicated time points by confocal microscopy as described above

Supplementary Material

Refer to Web version on PubMed Central for supplementary material.

Acknowledgments

We thank Brian Staskawicz for BS2, AvrBS2, and *Pst* strains with different Avr's and Maureen Hanson for cTP-GFP seeds. We thank Iris Meir for NES sequence suggestion and Amanda Carter for technical help during generation of *chup1*::NRIP1-Cerulean lines. This work was supported by NIH grant GM097587 (to S.P.D-K & J.L.C). Microscopy access was supported by an INBRE grant from NIH-NIGMS (P20 GM103446).

References

Al-Mehdi AB, Pastukh VM, Swiger BM, Reed DJ, Patel MR, Bardwell GC, Pastukh VV, Alexeyev MF, Gillespie MN. Perinuclear mitochondrial clustering creates an oxidant-rich nuclear domain required for hypoxia-induced transcription. Sci Signal. 2012; 5:ra47. [PubMed: 22763339]

Bae W, Lee YJ, Kim DH, Lee J, Kim S, Sohn EJ, Hwang I. AKR2A-mediated import of chloroplast outer membrane proteins is essential for chloroplast biogenesis. Nat Cell Biol. 2008; 10:220–227. [PubMed: 18193034]

Belousov VV, Fradkov AF, Lukyanov KA, Staroverov DB, Shakhbazov KS, Terskikh AV, Lukyanov S. Genetically encoded fluorescent indicator for intracellular hydrogen peroxide. Nat Methods. 2006; 3:281–286. [PubMed: 16554833]

Caplan J, Padmanabhan M, Dinesh-Kumar SP. Plant NB-LRR immune receptors: from recognition to transcriptional reprogramming. Cell Host Microbe. 2008a; 3:126–135. [PubMed: 18329612]

Caplan JL, Mamillapalli P, Burch-Smith TM, Czymmek K, Dinesh-Kumar SP. Chloroplastic protein NRIP1 mediates innate immune receptor recognition of a viral effector. Cell. 2008b; 132:449–462. [PubMed: 18267075]

Erickson JL, Ziegler J, Guevara D, Abel S, Klosgen RB, Mathur J, Rothstein SJ, Schattat MH. Agrobacterium-derived cytokinin influences plastid morphology and starch accumulation in Nicotiana benthamiana during transient assays. BMC Plant Biol. 2014; 14:127. [PubMed: 24886417]

Esau K. Anatomical and cytological studies on beet mosaic. J Agric Res. 1944; 69:95–117.

Hanson MR, Sattarzadeh A. Stromules: recent insights into a long neglected feature of plastid morphology and function. Plant Physiol. 2011; 155:1486–1492. [PubMed: 21330493]

Hanson MR, Sattarzadeh A. Trafficking of proteins through plastid stromules. Plant Cell. 2013; 25:2774–2782. [PubMed: 23983219]

Kadota A, Yamada N, Suetsugu N, Hirose M, Saito C, Shoda K, Ichikawa S, Kagawa T, Nakano A, Wada M. Short actin-based mechanism for light-directed chloroplast movement in Arabidopsis. Proc Natl Acad Sci USA. 2009; 106:13106–13111. [PubMed: 19620714]

Kohler RH, Cao J, Zipfel WR, Webb WW, Hanson MR. Exchange of protein molecules through connections between higher plant plastids. Science. 1997; 276:2039–2042. [PubMed: 9197266]

Krenz B, Jeske H, Kleinow T. The induction of stromule formation by a plant DNA-virus in epidermal leaf tissues suggests a novel intra- and intercellular macromolecular trafficking route. Front Plant Sci. 2012; 3:291. [PubMed: 23293643]

Kumar, A.; Dinesh-Kumar, SP.; Caplan, J. Stromules. In: Theg, S.; Wollman, F., editors. Adv Plant Biol: Plastid Biol. Vol. 5. 2014. p. 189-207.

Kwok EY, Hanson MR. In vivo analysis of interactions between GFP-labeled microfilaments and plastid stromules. BMC Plant Biol. 2004; 4:2. [PubMed: 15018639]

Lamb C, Dixon RA. The Oxidative Burst in Plant Disease Resistance. Annu Rev Plant Physiol Plant Mol Biol. 1997; 48:251–275. [PubMed: 15012264]

Leister RT, Dahlbeck D, Day B, Li Y, Chesnokova O, Staskawicz BJ. Molecular genetic evidence for the role of SGT1 in the intramolecular complementation of Bs2 protein activity in Nicotiana benthamiana. Plant Cell. 2005; 17:1268–1278. [PubMed: 15749757]

Liu Y, Ren D, Pike S, Pallardy S, Gassmann W, Zhang S. Chloroplast-generated reactive oxygen species are involved in hypersensitive response-like cell death mediated by a mitogen-activated protein kinase cascade. Plant J. 2007; 51:941–954. [PubMed: 17651371]

Liu Y, Schiff M, Marathe R, Dinesh-Kumar SP. Tobacco Rar1, EDS1 and NPR1/NIM1 like genes are required for N-mediated resistance to tobacco mosaic virus. Plant J. 2002; 30:415–429. [PubMed: 12028572]

Mansfiled J. From bacterial avirulence genes to effector functions via the hrp delivery system: an overview of 25 years of progress in our understanding of plant innate immunity. Mol Plant Pathol. 2009; 10:721–734. [PubMed: 19849780]

Mathur J, Barton KA, Schattat MH. Fluorescent protein flow within stromules. The Plant cell. 2013; 25:2771–2772. [PubMed: 23983222]

Mubarakshina Borisova MM, Kozuleva MA, Rudenko NN, Naydov IA, Klenina IB, Ivanov BN. Photosynthetic electron flow to oxygen and diffusion of hydrogen peroxide through the chloroplast envelope via aquaporins. Biochim Biophys Acta. 2012; 1817:1314–1321. [PubMed: 22421105]

Mur LA, Kenton P, Lloyd AJ, Ougham H, Prats E. The hypersensitive response; the centenary is upon us but how much do we know? J Exp Bot. 2008; 59:501–520. [PubMed: 18079135]

Natesan SK, Sullivan JA, Gray JC. Stromules: a characteristic cell-specific feature of plastid morphology. J Exp Bot. 2005; 56:787–797. [PubMed: 15699062]

Natesan SK, Sullivan JA, Gray JC. Myosin XI is required for actin-associated movement of plastid stromules. Mol Plant. 2009; 2:1262–1272. [PubMed: 19995729]

Oikawa K, Yamasato A, Kong SG, Kasahara M, Nakai M, Takahashi F, Ogura Y, Kagawa T, Wada M. Chloroplast outer envelope protein CHUP1 is essential for chloroplast anchorage to the plasma membrane and chloroplast movement. Plant Physiol. 2008; 148:829–842. [PubMed: 18715957]

Padmanabhan MS, Ma S, Burch-Smith TM, Czymmek K, Huijser P, Dinesh-Kumar SP. Novel positive regulatory role for the SPL6 transcription factor in the N TIR-NB-LRR receptor-mediated plant innate immunity. PLoS Pathogens. 2013; 9:e1003235. [PubMed: 23516366]

Schattat M, Barton K, Baudisch B, Klosgen RB, Mathur J. Plastid stromule branching coincides with contiguous endoplasmic reticulum dynamics. Plant Physiol. 2011; 155:1667–1677. [PubMed: 21273446]

Schattat MH, Griffiths S, Mathur N, Barton K, Wozny MR, Dunn N, Greenwood JS, Mathur J. Differential coloring reveals that plastids do not form networks for exchanging macromolecules. Plant Cell. 2012; 24:1465–1477. [PubMed: 22474180]

Schmidt von Braun S, Schleiff E. The chloroplast outer membrane protein CHUP1 interacts with actin and profilin. Planta. 2008; 227:1151–1159. [PubMed: 18193273]

Shalla TA. Assembly and Aggregation of Tobacco Mosaic Virus in Tomato Leaflets. J Cell Biol. 1964; 21:253–264. [PubMed: 14159028]

Shapiguzov A, Vainonen JP, Wrzaczek M, Kangasjarvi J. ROS-talk - how the apoplast, the chloroplast, and the nucleus get the message through. Front Plant Sci. 2012; 3:292. [PubMed: 23293644]

Sikorskaite S, Rajamaki ML, Baniulis D, Stanys V, Valkonen JP. Protocol: Optimised methodology for isolation of nuclei from leaves of species in the Solanaceae and Rosaceae families. Plant Methods. 2013; 9:31. [PubMed: 23886449]

Smith JM, Heese A. Rapid bioassay to measure early reactive oxygen species production in Arabidopsis leave tissue in response to living *Pseudomonas syringae*. Plant Methods. 2014; 10:6. [PubMed: 24571722]

Ting JP, Lovering RC, Alnemri ES, Bertin J, Boss JM, Davis BK, Flavell RA, Girardin SE, Godzik A, Harton JA, et al. The NLR gene family: a standard nomenclature. Immunity. 2008; 28:285–287. [PubMed: 18341998]

Torres MA, Jones JD, Dangl JL. Reactive oxygen species signaling in response to pathogens. Plant Physiol. 2006; 141:373–378. [PubMed: 16760490]

Vlot AC, Dempsey DA, Klessig DF. Salicylic Acid, a multifaceted hormone to combat disease. Annu Rev Phytopathol. 2009; 47:177–206. [PubMed: 19400653]

Wang C, Youle RJ. The role of mitochondria in apoptosis. Annu Rev Genet. 2009; 43:95–118. [PubMed: 19659442]

Zurbriggen MD, Carrillo N, Hajirezaei MR. ROS signaling in the hypersensitive response: when, where and what for? Plant Signal Behav. 2010; 5:393–396. [PubMed: 20383072]

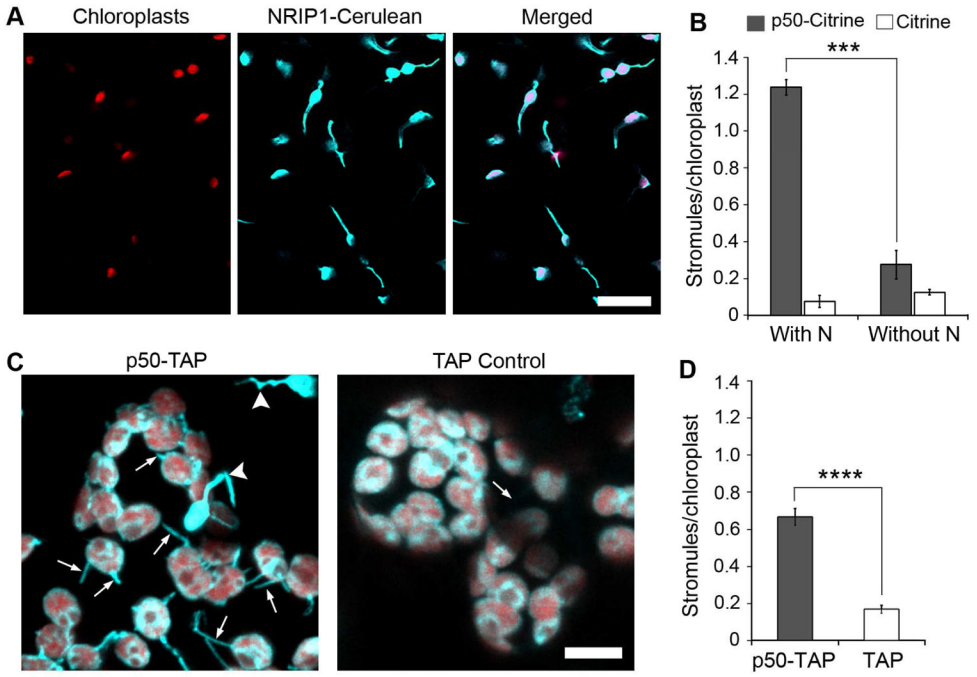

Figure 1. Induction of stromules during viral effector activated HR-PCD

A. Transient expression of p50 fused to a tandem affinity purification tag (TAP) for approximately 46 h in N-containing NRIP1-Cerulean (blue) *N. benthamiana* plants induces stromules (arrows) in epidermal chloroplasts (red autofluorescence). Scale bar equals 10 μm.

B. Expression of p50-Citrine in N plants resulted in strong increase in stromules per chloroplast compared to Citrine alone in N plants and p50-Citrine or Citrine in plants without N. Data represented as the mean ± standard error of the mean (SEM), ***P<0.005 (Student's *t*-test).

C. Transient expression of p50-TAP (left panel) for approximately 46 h in N-containing NRIP1-Cerulean (blue) *N. benthamiana* plants induces stromules (arrows) in mesophyll chloroplasts (red autofluorescence) compared to TAP alone control (right panel). Stromules originating from epidermal chloroplasts have a higher level of NRIP1-Cerulean fluorescence (arrowheads) and are smaller than mesophyll chloroplasts. Scale bar equals 10 μm.

D. Quantification of stromules from experiments described in C shows increased stromules in p50-TAP expressing plants compared to the TAP alone control. Data represented as the mean ± SEM, ****P<0.001 (Student's *t*-test).

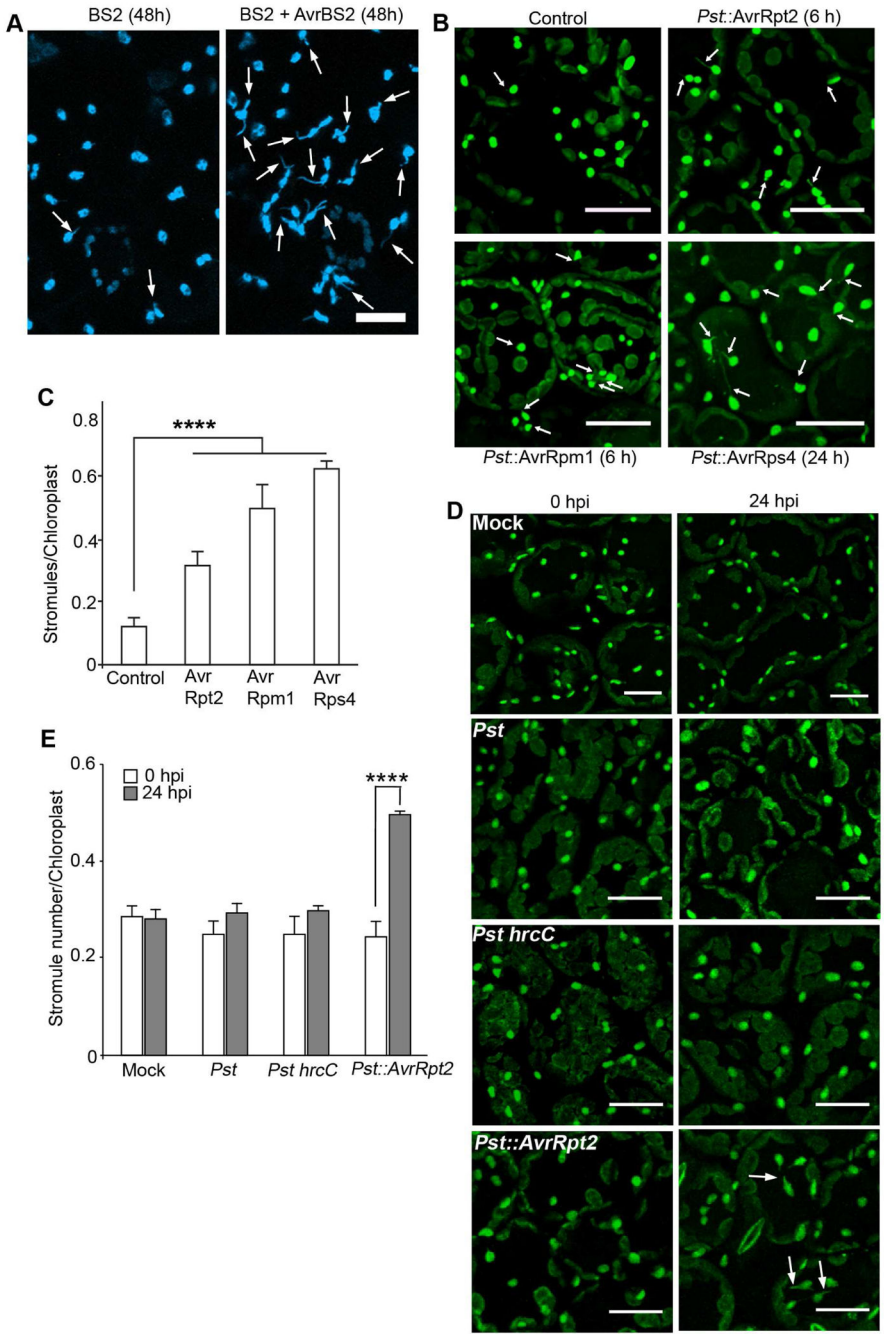

Figure 2. Stromule induction during bacterial immunity

A. Stromules (arrows) were induced in transgenic NRIP1-Cerulean (blue) *N. benthamiana* plants after 48 h of transient coexpression of BS2 with AvrBS2 (right panel) compared to BS2 control (left panel). Scale bar equals 10 μm.

B. NRIP1-Cerulean (green) expressing transgenic Col-0 Arabidopsis plants were infiltrated with 1×10^6 cfu/ml *Pseudomonas syringae pv tomato* DC3000 (*Pst)* expressing different effectors. Increased number of stromules (arrows) was observed in plants infected with *Pst::AvrRpt2* for 6 h (top right panel), *Pst::AvrRpm1* for 6 h (bottom left panel), and

Pst::AvrRps4 for 24 h (bottom right panel) compared to the mock control (top left panel). Scale bar equals 25 μm.

C. Quantification of stromules from experiments described in B shows increased stromules in plant infected with *Pst::AvrRpt2*, *Pst::AvrRpm1*, and *Pst::AvrRps4* compared to the mock control. Data represented as the mean ± SEM, ****P<0.001 (Student's *t*-test).

D. *Pst* and *Pst hrcC* strains at 2.5×10^5 cfu/ml were infiltrated onto NRIP1-Cerulean *Arabidopsis* plants (green). Stromules were not induced in plants infected with *Pst* or *Pst hrcC* or mock control (top 3 panels) compared to plants infected with *Pst::AvrRpt2* (bottom right panel). Scale bar equals 20 μm.

E. Quantification of stromules from experiments described in D shows similar number of stromules in *Pst* and *Pst hrcC* infected plants to that of mock control. *Pst::AvrRpt2* infection induced significant stromules. Data represented as the mean ± SEM, ****P<0.001 (Student's *t*-test).

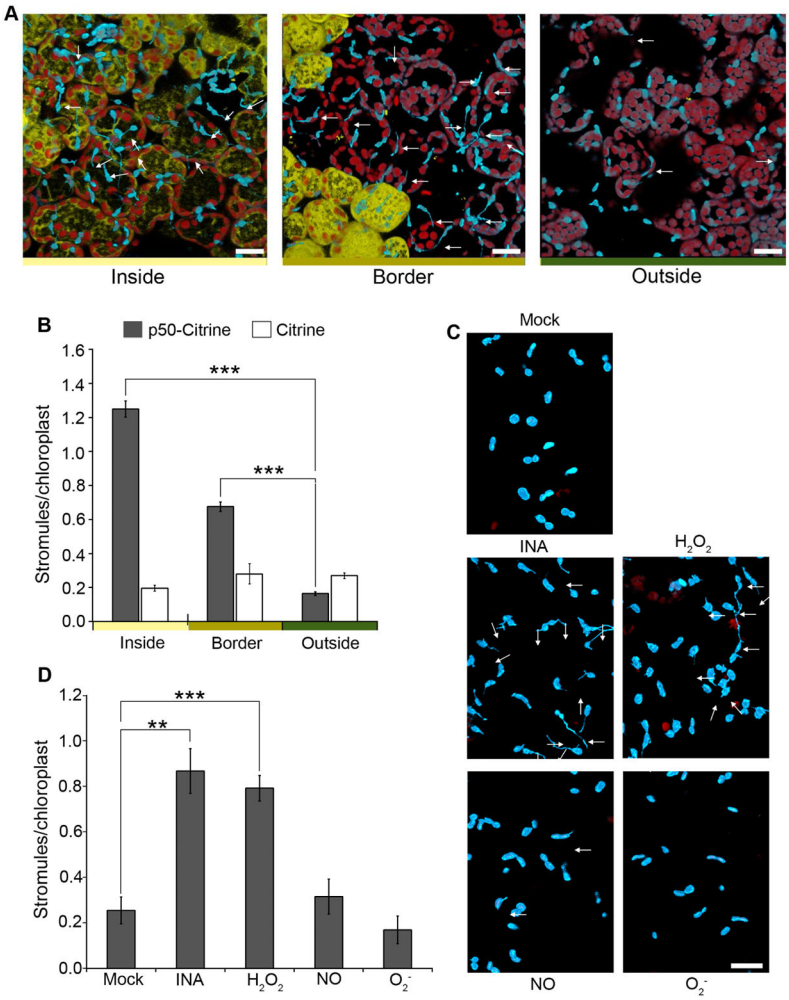

Figure 3. Stromules are induced at and along the border of HR-PCD and by exogenous application of H_2O_2 and SA

A. The initial HR-PCD site was marked by transient expression of p50-Citrine (46 h; yellow). Citrine was used as a negative control. 46 h post-expression of p50-Citrine, strong stromule induction (arrows) was observed inside the HR-PCD site (left), a moderate stromule induction was observed along the border of the HR-PCD site (middle), and background amount stromules was observed away from the HR-PCD site (right). Scale bar equals 10 μm.

B. Quantification of stromules from experiments described in A shows strong induction of stromules inside the p50-Citrine induced HR-PCD site (gray bars), a moderate induction along the border and no induction outside HR-PCD site compared to the Citrine control (white bars).. Data represented as the mean ± SEM, ***P<0.005 (Student's *t*-test).

C. Stromules (arrows) were induced in NRIP1-Cerulean *N. benthamiana* transgenic plants upon exogenous application of SA analog INA and H_2O_2 (middle panels) compared to NO donor SNAP, O_2^- generated by xanthine with xanthine oxidase (bottom panels), and mock buffer control (top panel) that did not cause stromule induction. Scale bar equals 10 μm.

D. Qunatification of stromules from experiments described in C shows increased stromule induction in INA or H_2O_2 treatments compared to NO, O_2, or mock buffer control. Data represented as the mean ± SEM, **P<0.01, ***P<0.005 (Student's *t*-test).

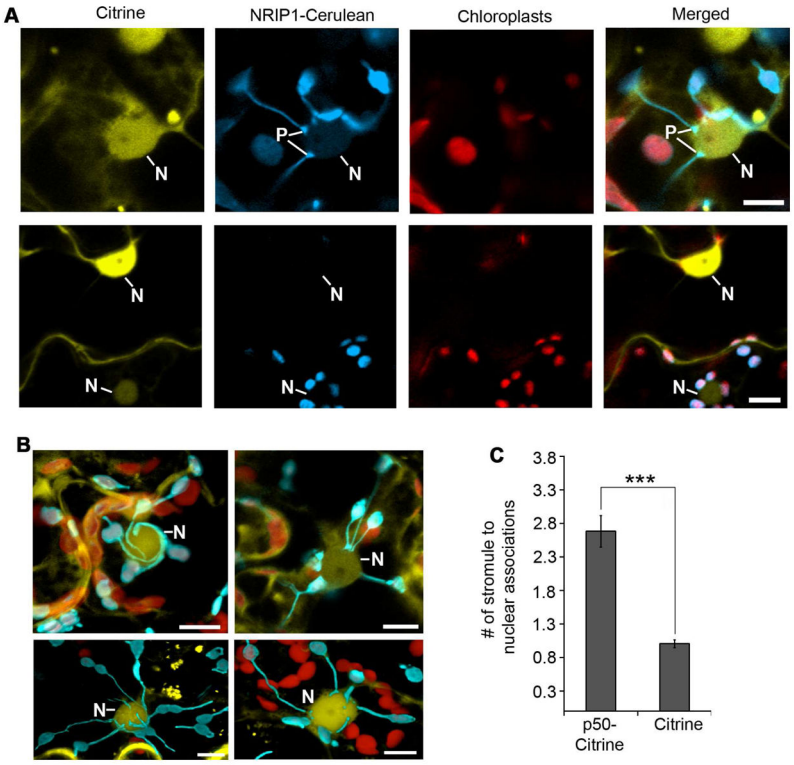

Figure 4. Induction of chloroplast stromule-to-nuclear connections during HR-PCD

A. Transient expression of p50-Citrine (top panels) in N-containing NRIP1-Cerulean plants was used to monitor stromule-to-nuclear connections during HR-PCD. Expression of Citrine was used as a no HR-PCD control (bottom panels). Stromules were observed connecting to nuclei (N) with pad-like structures (P) at the points of contact (top panels) between stromules and nucleus. The larger chloroplasts (red) are located in mesophyll cells and contained very few stromules. Scale bars equal 10 μm.

B. During p50-mediated HR-PCD, confocal micrographs show stromules wrapped around nuclei (top left panel, maximum intensity projection of a z-stack). There were also clusters of stromule tip connections directly to the nucleus (top right panel, single plane of a z-stack) and nuclei with a mixture of tip or surrounding stromule connections (bottom panels, transparent projections of z-stacks). Scale bars equal 10 μm.

C. Stromule-to-nuclei connections were manually enumerated from 3D confocal microscopy z-stacks. There was an increase in stromule-to-nuclei connections per chloroplast during p50-Citrine-initiated HR-PCD compared to Citrine, the no HR-PCD control. Data represented as the mean ± SEM,***P<0.005 (Student's *t*-test).

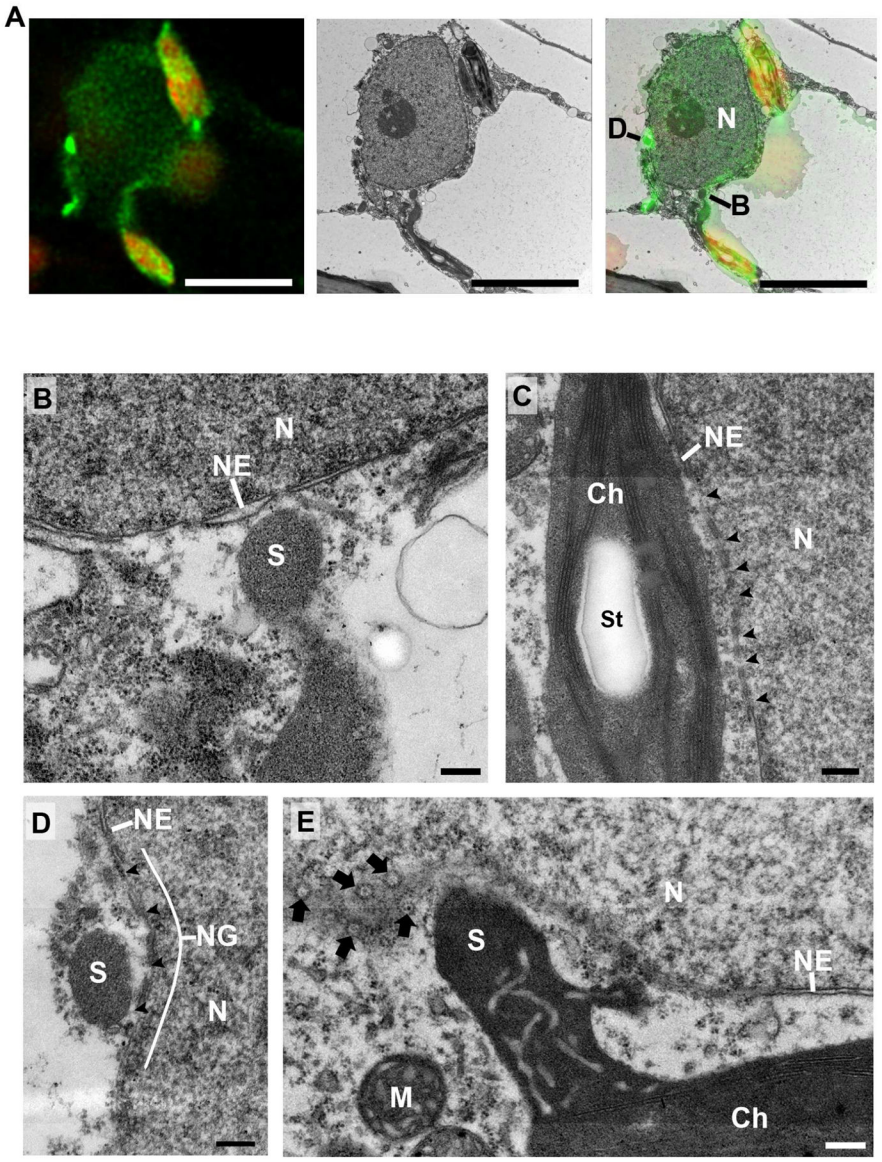

Figure 5. Correlative light and electron microscopy of chloroplast-to-nuclear connections induced during HR-PCD

A. Stromules were induced by transient expression of p50-Citrine in NRIP1-Cerulean expressing N plants. Confocal z-stack images were acquired and deconvolved (left). Chloroplasts (red) have stromules (green) extending to and around the nucleus. A transmission electron micrograph of the exact same nucleus was imaged (middle). The confocal and TEM micrographs were overlaid (right) to determine the location and type of chloroplast-to-nuclear connections. An approaching stromule connection (B) and a cross-section through surrounding chloroplasts (D) were identified and examined at higher magnification and shown in panels B and D. Scale bars equal 5 μm.

B. The tips of stromules are in close contact, but the outer membrane and nuclear membrane do not directly associate. There appears to be cytosol between the stromule (S) and nucleus

(N). A break or pore was observed where the tip of a stromule (S) approached the nuclear envelope (NE). Scale bar equals 0.2 μm.

C. The body of chloroplasts (Ch) often can be found in close association with nuclei (N). Numerous nuclear envelope (NE) perforations (arrowheads) were observed at the junction of the body of chloroplasts. St, starch inside the chloroplast. Scale bar equals 0.2 μm.

D. A stromule (S) wrapped around a nucleus (N) was found in nuclear groove (NG) that increased stromule contact with the nuclear envelope (NE). There were perforations (arrowheads) in the nuclear envelope of the nuclear groove. Scale bar equals 0.2 μm.

E. Oblique sections through a stromule (S)-to-nuclear (N) connection reveal numerous nuclear pores (arrows) in the nuclear envelope (NE) in close proximity to the connection. M, mitochondria near chloroplast. Scale bar equals 0.2 μm.

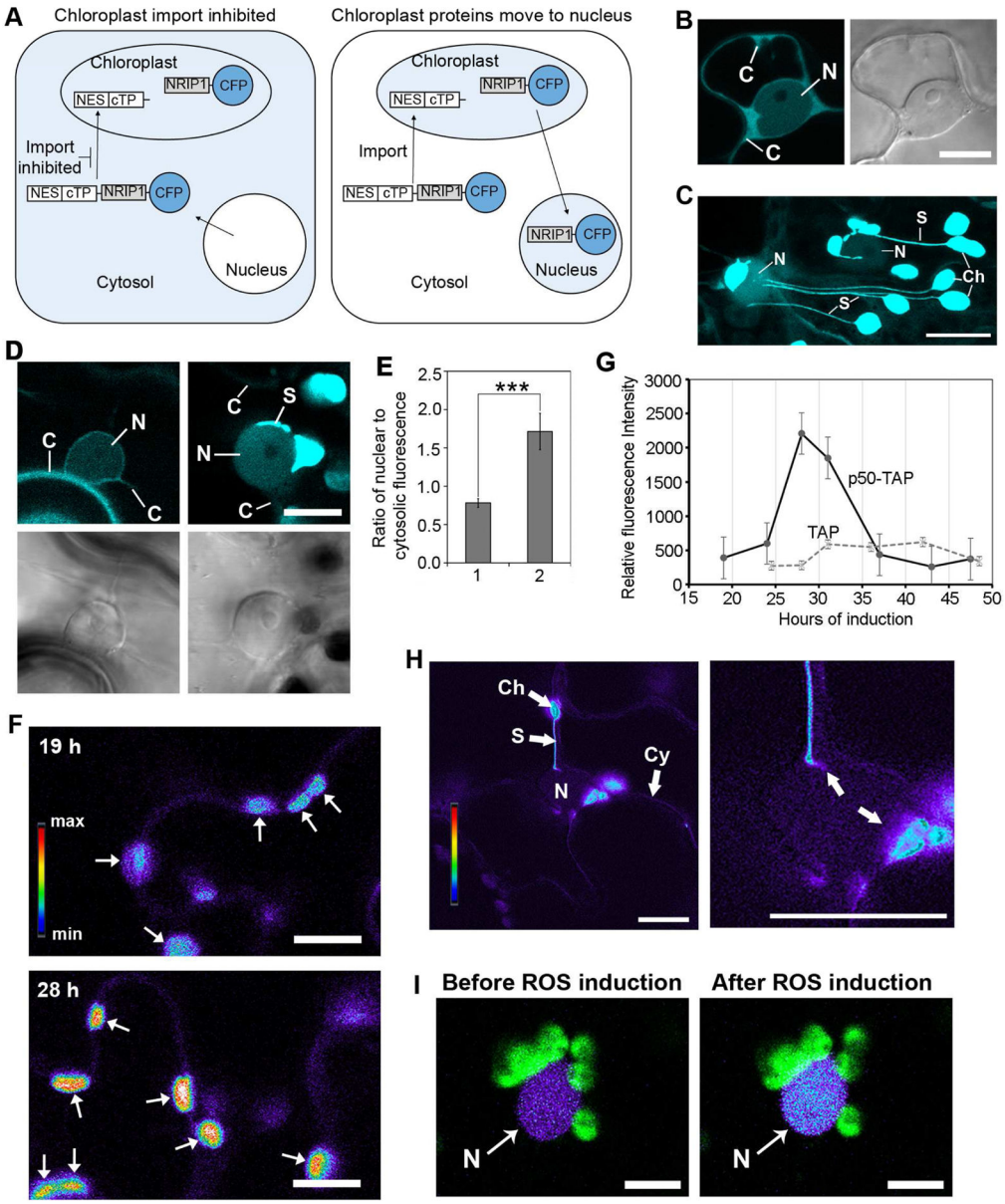

Figure 6. Movement of NRIP1 and H_2O_2 from chloroplast to nucleus

A. Schematic of experimental strategy used to demonstrate that NRIP1-Cerulean moves out of chloroplasts and accumulates in the nucleus. Nuclear export sequence (NES) from HIV REV was fused to the amino-terminus of NRIP1-Cerulean. Processing of NES-NRIP1-Cerulean that is imported into the chloroplasts will cleave off NES with the chloroplast transit peptide (cTP) (right panel). In this case, movement of NRIP1-Cerulean to the nucleus will results in increased Cerulean fluorescence in the nucleus (right panel). If import of NES-NRIP1-Cerulean into chloroplasts is inhibited, NES in the NES-NRIP1-Cerulean would be retained in the cytosol because of NES (left panel).

B. NES is functional. Transient expression of NES fused to Cerulean alone (NES-Cerulean) in *N. benthamiana* plants results in exclusion of Cerulean fluorescence from the nucleus (N) and increased fluorescence in the cytosol (C). Scale bar equal 10 μm.

C. Addition of NES to NRIP1-Cerulean does not disrupt localization to the chloroplasts. NES-NRIP1-Cerulean was transiently expressed in *N. benthamiana* leaves. After 46 h of expression, leaf sections were imaged by confocal microscopy. Strong Cerulean fluorescence was observed in the chloroplasts (Ch) and stromules (S). N, nucleus. Scale bar equal 10 μm.

D. Chloroplast-localized NRIP1 moves out of chloroplasts to nuclei. NES-NRIP1-Cerulean and Cerulean-NRIP1(cTP)-NES were separately coexpressed with p50-TAP in N-containing plants. After 36 h, increased Cerulean fluorescence was observed in the nucleus (N) of cells expressing NES-NRIP1-Cerulean, (right panels); C, cytosol. The very bright signal is a stromule (S) connected to the nucleus (right panel). In Cerulean-NRIP1(cTP)-NES control, the Cerulean fluorescence was largely excluded from the nucleus (N) resulting in increased fluorescence in the cytosol (C) (left panels). Top panels, confocal images; bottom panels, differential interference contrast (DIC) images. Scale bar equal 10 μm.

E. Quantification shows NES-NRIP1-Cerulean (2) expressing cells with high ratio of nuclear-to-cytosolic Cerulean fluorescence compared to the control Cerulean-NRIP1(cTP)-NES (1). Data represented as the mean ± SEM,***P<0.005 (Student's *t*-test).

F. Visualization of increase in H_2O_2 in the chloroplasts using the HyPer H_2O_2 sensor. Chloroplast-targeted RecA(cTP)-HyPer and p50-TAP were transiently co-expressed in N plants for 19 to 48 h. Images are a ratio of green fluorescence excited by either a 405 nm or 514 nm laser. For display, the ratio was multiplied by 300 and a rainbow 2 lookup table was applied in Zen 2012. Higher levels of ROS in chloroplasts observed at 28 h post induction of defense responses by p50-TAP (bottom panel) compared to 19 h post induction (top panel). Scale bar equals 10 μm.

G. RecA(cTP)-HyPer was used to examine chloroplast-generated ROS during a time course of p50-TAP-induced defense responses. The ROS burst peaked at approximately 28 h of expression of p50-TAP compared to the TAP control.

H. Transient expression of the RecA(cTP)-HyPer H_2O_2 sensor in the chloroplasts (Ch), nucleus (N) and cytosol (Cy) of *N. benthamiana* plants. Images are a ratio of fluorescence emitted by excitation with a 405 nm or 514 nm laser that reflects H_2O_2 concentration and displayed using a rainbow 2 lookup table. Increased H_2O_2 in the nucleus was seen at association sites between stromules and the main body of the chloroplast (right panel, arrows). Right panel is higher magnification image. Scale bars equal 10 μm.

I. Increase in H_2O_2 in the nucleus. Nuclear-targeted NLS-HyPer was transiently expressed in *N. benthamiana* leaves. Chloroplasts (green) in close association with nuclei (N) were scanned with a 405 nm laser to generate light induced ROS in chloroplasts. An increase in ROS in the nucleus was observed (right panel) after ROS induction in the chloroplasts. Scale bars equal 10 μm.

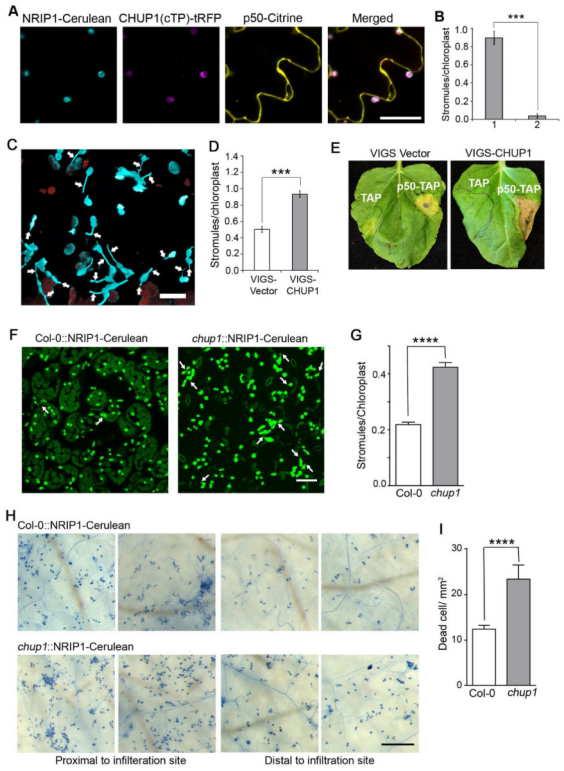

Figure 7. Constitutive induction of stromules enhances HR-PCD

A. p50-Citrine (yellow, top right) and CHUP1(cTP)-tRFP (magenta, bottom left) were transiently coexpressed in NRIP1-Cerulean (blue, top left) transgenic *N. benthamiana* leaves. CHUP1(cTP)-tRFP colocalized with NRIP1-Cerulean in chloroplasts (merged) and completely disrupted p50-Citrine induced stromule formation. Scale bars equal 10 μm.

B. Stromules from experiment described in A were quantified from 2D maximum intensity projections of confocal microscopy z-stacks. Stromules were induced in plants expressing p50-Citrine (1) but significantly reduced in plants co-expressing p50-Citrine and CHUP1(cTP)-tRFP (2). Data represented as the mean ± SEM, ***P<0.005 (Student's *t*-test).

C. Confocal micrograph showing that virus induced gene silencing (VIGS) of *CHUP1* in N-containing plants induces stromules (arrows) constitutively. Scale bar equals 10 μm.

D. The number of stromules per chloroplast was higher in VIGS-*CHUP1* plants compared to the VIGS-Vector control. Data represented as the mean ± SEM, ***P<0.005 (Student's *t*-test).

E. After 3 days post p50-TAP expression, HR-PCD was observed as yellowing and limited brown, cellular collapse in the VIGS vector control. In the VIGS-*CHUP1* plants, HR-PCD was accelerated as complete brown, cellular collapse. TAP was used as a negative control.

F. Constitutive induction of stromules (arrows) was observed in Arabidopsis *chup1* knockout plants (right panel) compared to Col-0 wild type plants (left panel). Scale bar equals 20 μm.

G. Quantification of data from D shows increased stromules per chloroplast in *chup1* plants compared to the Col-0 control. Data represented as the mean ± SEM, ****P<0.001 (Student's *t*-test).

H. Col-0 (upper panels) and *chup1* (bottom panels) plant leaves were infiltrated with $1X10^6$ Cfu/ml *Pst::AvrRpt2* and stained with trypan blue 6 h post-infection. Two independent representative images of close to the infiltration site (left panels) and distal to the infiltration site (right panels) are shown. *chup1* plants show increased cell death compared to the Col-0. Scale bar equals 0.5mm.

I. Quantification of dead cells in experiments described in F shows increased cell death in *chup1* compared to Col-0. Data represented as the mean ± SEM, ****P<0.001 (Student's *t*-test).